ISSN 2321-807X
Volume 12 Number23
Journal of Advances in chemistry

High Performance of CSI Fed IM Drives at Low Speed operation with MRAS Based Estimation of Stator Resistance

[1]N.Panneer selvam, [2]V.Rajasekaran
[1] M.A.M. Polytechnic College, Trichy, Tamil Nadu, INDIA
Email: knpselvam@gmail.com
[2] PSNA College of Engineering& Technology, Dindigul, Tamil Nadu, INDIA
Email: rajasekaran_v@yahoo.com

ABSTRACT

This paper is proposed to improve the performance of sensorless vector controlled CSI fed induction motor drives during low-speed operations. In general the performance of sensorless vector controlled induction motor drives is poor at very low speed due to stator resistance variations and the estimated flux and torque deviates from its set value. Therefore online tuning of the stator resistance is necessary at very low speed. The performance and efficiency of an induction motor drive system can be enhanced by online tuning of stator resistance. A novel model reference adaptive system (MRAS)-based algorithm for simultaneous identification of stator resistance (R_s) and rotor speed ($\boldsymbol{\omega}_r$) implemented in sensorless Field oriented controlled CSI fed induction motor. The reference model and adjustable model are interchangeable for concurrent $\boldsymbol{\omega}_r$ and R_s estimation in the low-speed operating region is investigated. The simulation and experimental results are proved that the proposed method is improving the performance of the drive system at low speed operation.

KEY WORDS

Current source inverter, Induction Motor, Sensorless Speed, MRAS, Resistance tuning.

INTRODUCTION

Induction motor drives are widely used in industries due to its advantages of simple construction, easy operation; less maintenance and high efficiency etc. Variable speed Induction motor drive is greatly increased in industry for various applications. The current-source inverter (CSI) is well suited for medium-voltage drives applications compared with VSI fed drives due to following advantages

- Simple converter structure,
- Motor-friendly waveforms,
- Inherent four-quadrant operation capability,
- Reliable short-circuit protection.

The current source inverter fed Induction motor drive block diagram shown in Fig.1, a DC link inductor is connected between current source inverter and controlled rectifier to limit the DC link current. To improve the performance of CSI fed drive the maximum modulation index control scheme introduced [1] to regulate the DC link current, reduce the dynamic over voltage the Integrated Gate Commutated Thyristor (IGCT) is used in CSI fed IM drives [2] and SGCT is viable and has significant advantages of PWM CSI fed drives [3] and solve the power factor problem [4].

Different control strategies are employed in the high-power current-source drives to improve the system dynamics and reliability. The Space vector control [5], reduce the switching losses by PWM technique [6], increase the efficiency [7]. The concept of vector control for CSI fed high-performance induction motor drive systems realized in rotor flux oriented control with PWM [8] & [9], IFOC [10], and direct torque control [11] & [12] has become very popular during the last decades.

Vector control techniques have been separated into two categories, such as direct and indirect control schemes. Both methods require the knowledge of machine parameters. Indirect control schemes require knowledge of the machine inductances as well as the rotor time constant, while in direct schemes only the stator resistance value has to be known for flux estimation. Depending on the specific method, these parameters are highly affecting the flux vector calculation precision since these parameters are varied during low speed operation. In high speed range there is no estimation error in stator flux. But in low-speed operation, the stator resistance value becomes critical for the calculations due to temperature variations and a stator flux will produce a significant estimation error. An accurate value of the stator resistance is necessary for correct operation of a sensor less drive in the low speed region. If any mismatch between the actual value and the value the system become unstable. As a consequence, numerous on-line schemes for stator resistance estimation have been proposed in recent past decades [13]-[18]. A MRAS based on-line identification of stator resistance and speed estimation for a sensor less rotor-flux-oriented (FOC) vector-controlled CSI fed induction motor drive is proposed with combines ideas of [18]-[20]. Stator resistance estimation is developed in combination with the rotor flux based MRAS speed estimator and it operates in the stationary reference frame utilize the idea of [16]-[18] related to the creation of the error quantity for adaptive stator resistance identification. The error quantity is formed on the basis of differences in rotor flux component values, obtained at the output of the reference and the adjustable model. The observation of [19] & [20] that the role of the reference and the adjustable model is interchangeable for the purposes of speed and stator resistance estimation in parallel. This difference is made possible by the observation that the MRAS speed estimator utilizes an error quantity related to the instantaneous phase difference between the two estimates of the rotor flux. The same error quantity was used [19] & [20] for stator resistance estimation. In this paper section II described the basic control of FCO with CSI fed IM drives. A detailed derivation of the parallel rotor speed and stator resistance estimation algorithms is provided in section III of this paper and the proposed scheme is verified by MATLAB/SIMULINK software and experimentally in section IV and the validity of the proposed method is verified.

CURRENT SOURCE INVERTER DRIVE SYSTEM AND ITS CONTROL SCHEME

Fig.1 illustrates the block diagram of a current source drive system and its FOC control scheme. The current source drive consists of an input LC filter, a PWM CSR, a dc link choke, a PWM CSI and an output filter capacitor. A high power induction motor is connected at the output of the drive. A bridge configuration is usually used for both the rectifier and the inverter, with which the drive system can be used for medium voltage applications. The drive's input and output filter capacitors are required to assist the commutation of switching devices, while they can also attenuate unwanted harmonics. The dc choke between the CSR and CSI is used to smooth the dc current. It also prevents the dc current from a sudden increase in case of short-circuit fault and thus provides sufficient time for the protection circuit to function. The FOC scheme for the current source drive system is based on the rotor flux orientation and the decoupled control of the motor flux and torque provides improved dynamics and stability. For the rotor flux estimation, voltage model rotor flux identification method (using the motor stator voltage and current) combined with a current model method (using the stator current and the rotor speed) is implemented for an optimal system performance. The current model method can estimate the rotor flux precisely at low rotor speeds with the stator frequency of a few Hertz.

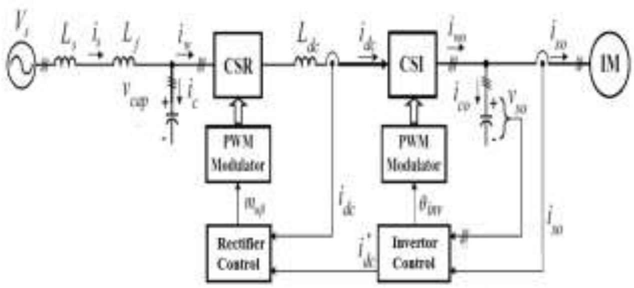

Fig.1 Field oriented control Current source inverter drive system

BASIC SPEED ESTIMATOR AND VECTOR CONTROL SCHEME

The basic MRAS speed estimator is originally proposed in [20] and illustrated in Fig. 2. Equation (1) represents the reference (voltage) model and equation (2) represent the adjustable (current) models are derived from the stator quantities like voltage and currents. The estimator operates in the stationary reference frame ($\boldsymbol{\alpha}$,) and it is described with the following equations [20]:

$$p\underline{\hat{\Psi}}_{rV}^{s} = \frac{L_m}{L_r}\left[\underline{u}_s^s - \left(\hat{R}_s + \sigma L_s p\right)\underline{i}_s^s\right] \quad (1)$$

$$p\underline{\hat{\Psi}}_{rI}^{s} = \frac{L_m}{T_r}\underline{i}_s^s - \left(\frac{1}{T_r} - j\hat{\omega}\right)\underline{\hat{\Psi}}_{rI}^{s} \quad (2)$$

$$\hat{\omega} = \left(K_{p\omega} + \frac{K_{I\omega}}{p}\right)e_\omega \quad (3)$$

$$e_\omega = \underline{\hat{\Psi}}_{rI}^{s} \times \underline{\hat{\Psi}}_{rV}^{s} = \hat{\Psi}_{\alpha rI}\hat{\Psi}_{\beta rV} - \hat{\Psi}_{\beta rI}\hat{\Psi}_{\alpha rV} \quad (4)$$

A symbol ^ denotes in (1) - (4) estimated quantities, symbol '*p*' stands for *d*/*dt*, T_r is the rotor time constant and $\sigma = 1 - L_m^2/L_sL_r$. All the parameters in the motor and the estimator are assumed to be the same value, except for the stator resistance (hence a hat above the symbol in (1)). Underlined variables are space vectors, and sub-scripts *V* and *I* stand for the outputs of the voltage (reference) and current (adjustable) models, respectively. Voltage, current and flux are denoted with *u*, *i* and ψ, respectively, and subscripts *s* and *r* stand for stator and rotor, respectively. Superscript's' in space vector symbols denote the stationary reference frame.

From the evident (1)-(4) and Fig. 2, the adaptive mechanism (PI controller) relies on an error quantity that represents the difference between the instantaneous positions of the two rotor flux estimates. The second degree of freedom, the difference in amplitudes of the two rotor flux estimates, is not utilized. The parallel rotor speed and stator resistance MRAS estimation scheme, which will be developed in the next section, will make use of this second degree of freedom to achieve simultaneous estimation of the two quantities. The role of the reference and the adjustable model will be interchanged for this purpose, since the rotor flux estimate of (2) is independent of stator resistance.

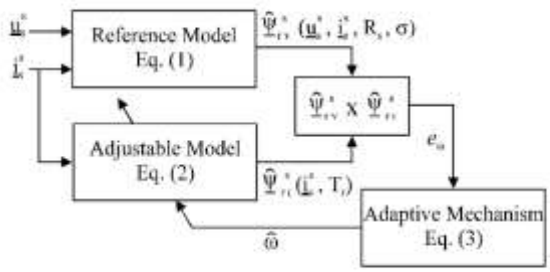

Fig. 2. Basic configuration of the rotor flux based MRAS speed estimator

IMPACT OF FILTER CAPACITOR ON SYSTEM CONTROL

CSI-fed motor drives have filter capacitors connected at the output of the inverter. This means that a portion of the inverter currents goes through the capacitors. The weight of the filter capacitors on the system control is investigated in this section. The inverter reference currents can be expressed as follows [20]:

$$i_{dw}^{*} = i_{cd} + i_{ds}^{*}$$
$$i_{qw}^{*} = i_{cq} + i_{qs}^{*} \qquad (5)$$

Where i_{cd} and i_{cq} are the estimated capacitor *d*, *q*-axis currents are usually simplified as follows to reduce the sensitivity and noise caused by the derivative terms:

$$i_{cd} = -\omega_e v_{qs} C_f$$
$$i_{cq} = \omega_e v_{ds} C_f \qquad (5a)$$

Where C_f , ω_e , v_{ds}, and v_{qs} are the inverter-side filter capacitance, motor electrical angular frequency, and stator *d*-axis and *q*-axis voltages, respectively.

The induction motor control scheme is shown in Fig. 3, where rotor flux orientation is employed [20]. It includes, apart from a speed controller, rotor flux and torque controllers as well. The required feedback quantities for the torque and rotor flux are obtained from the reference model (1). The flux and speed controllers are utilized to generate the reference *d*-axis current (i_{ds}^{*}) and *q*-axis current (i_{qs}^{*}), respectively. This reference currents and the compensated capacitor currents are used to produce the i_{qw}^{*} and i_{dw}^{*} (Eq (5)) in order to minimize the dc-link current. the amplitude (i_{dc}^{*}) Of the synthesized inverter reference current has served as the reference for dc-link current control of the current source rectifier, while the corresponding phase θ_w is added to the rotor flux angle θ_f for the modulation of the CSI. The current model is utilized for the flux estimation

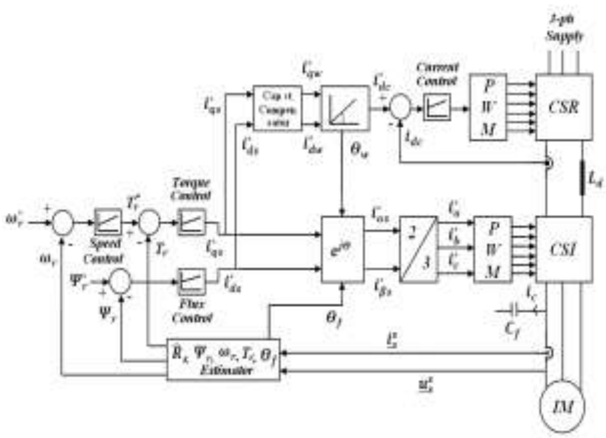

Fig. 3. Structure of the speed sensor less current-fed rotor flux oriented induction motor drive

PARALLEL STATOR RESISTANCE AND ROTOR SPEED ESTIMATION

In this section the proposed parallel rotor speed and stator resistance estimation scheme is designed based on the concept of hyper stability [20] in order to make the system asymptotically stable. For the purpose of deriving an adaptation mechanism, it is valid to initially treat rotor speed as a constant parameter, since it changes slowly compared to the change in rotor flux. The stator resistance of the motor varies with temperature, but variations are slow so that it can be treated as a constant parameter, too. Fig. 4 show that the configuration of the proposed method to estimate rotor speed and stator resistance in parallel.

Let R_S and $\boldsymbol{\omega}_r$ denote the true values of the stator resistance in the motor and rotor speed, respectively. These values are different from the estimated values. Consequently, a mismatch between the estimated and true rotor flux space vectors appears as well. The error equations for the voltage and the current model outputs can then be written as

$$p\underline{\varepsilon}_V = -\frac{L_r}{L_m}\left(R_s - \hat{R}_s\right)\underline{i}_s^s \qquad (6a)$$

$$\underline{\varepsilon}_V = \underline{\Psi}_{rV}^s - \underline{\hat{\Psi}}_{rV}^s = \varepsilon_{\alpha V} + j\varepsilon_{\beta V} \qquad (6b)$$

$$p\underline{\varepsilon}_I = \left(j\omega - \frac{1}{T_r}\right)\underline{\varepsilon}_I + j(\omega - \hat{\omega})\underline{\hat{\Psi}}_{rI}^s \qquad (6c)$$

$$\underline{\varepsilon}_I = \underline{\Psi}_{rI}^s - \underline{\hat{\Psi}}_{rI}^s = \varepsilon_{\alpha I} + j\varepsilon_{\beta I} \qquad (6d)$$

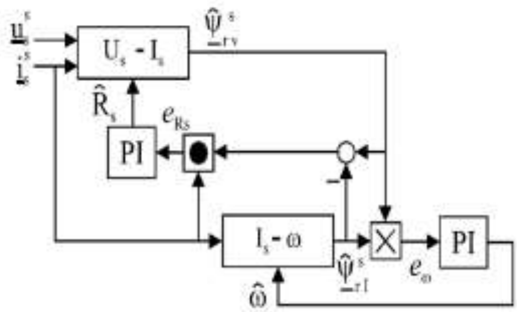

Fig. 4. Proposed MRAS based parallel estimation of rotor speed and stator resistance.

Symbols $\underline{\Psi}_{rV}^s$. $\underline{\Psi}_{rI}^s$ in (6b), (6b) stand for the true values of the two rotors flux space vectors. Equations (6a)-(6d) can be rewritten in matrix notation as

$$p\begin{bmatrix}\varepsilon_{\alpha I}\\ \varepsilon_{\beta I}\\ \varepsilon_{\alpha V}\\ \varepsilon_{\beta V}\end{bmatrix} = \begin{bmatrix}-\frac{1}{T_r} & -\omega & 0 & 0\\ \omega & -\frac{1}{T_r} & 0 & 0\\ 0 & 0 & 0 & 0\\ 0 & 0 & 0 & 0\end{bmatrix}.\begin{bmatrix}\varepsilon_{\alpha I}\\ \varepsilon_{\beta 1}\\ \varepsilon_{\alpha V}\\ \varepsilon_{\beta V}\end{bmatrix} - W = A\underline{\varepsilon} - W \qquad (7)$$

Where W is the nonlinear block, defined as follows:

$$W = \begin{bmatrix}-\Delta\omega & \begin{bmatrix}0 & -1\\ 1 & 0\end{bmatrix} & 0 & 0\\ 0 & 0 & 0 & 0\\ 0 & 0 & \frac{L_r}{L_m}\Delta R_s & \begin{bmatrix}1 & 0\\ 0 & 1\end{bmatrix}\end{bmatrix}\begin{bmatrix}\hat{\Psi}_{\alpha rI}\\ \hat{\Psi}_{\beta rI}\\ i_{\alpha s}\\ i_{\beta s}\end{bmatrix} \qquad (8)$$

$$W = \begin{bmatrix}-\Delta\omega J & 0\\ 0 & \frac{L_r}{L_m}\Delta R_S I\end{bmatrix}.\begin{bmatrix}\hat{\Psi}_{rI}^S\\ i_s^S\end{bmatrix}$$

Here $\Delta\omega = \omega - \hat{\omega}$,

$\Delta R = R_s - \hat{R}_s \quad \Psi_{rI}^S = \left[\hat{\Psi}_{\alpha rI} \quad \hat{\Psi}_{\beta rI}\right]^T$,

$i_s^S = [i_{\alpha s} \quad i_{\beta s}]^T, \quad J = \begin{bmatrix}0 & -1\\ 1 & 0\end{bmatrix}$

$and\ \mathrm{I} = \begin{bmatrix}1 & 0\\ 0 & 1\end{bmatrix}$

The system is hyper stable if the input and output of the nonlinear block W satisfy Popov's criterion [20]:

$S = \int_0^{t_1} \underline{\varepsilon}^T . W dt \geq \gamma^2 . \forall t_1$ (9)

Where, using (8)

$\underline{\varepsilon}^T . W = -\Delta\omega \left(\underline{\varepsilon}_I^T . J . \hat{\Psi}_{rI}^s \right) + \frac{L_r}{L_m} \Delta R_S \left(\underline{\varepsilon}_V^T . i_s^s \right)$ (10)

Substitution of (10) into (9) yields

$$S = \int_0^{t_1} \underline{\varepsilon}^T . W dt = \underbrace{- \int_0^{t_1} \Delta\omega \left(\underline{\varepsilon}_I^T . J . \hat{\Psi}_{rI}^s \right) dt}_{S_1} + \underbrace{\frac{L_r}{L_m} \int_0^{t_1} \Delta R_S \left(\underline{\varepsilon}_V^T . i_s^s \right) dt}_{S_2}$$

$s = S_1 + \frac{L_r}{L_m} . S_2 \geq -\gamma^2 . \forall t_1$ (11)

The validity of (11) can be verified by means of inequalities (12) and (13) with adaptive mechanisms given in (14), (15) for rotor speed estimation and stator resistance identification, respectively:

$S_1 = -\int_0^{t_1} \Delta\omega \left(\underline{\varepsilon}_I^T . J . \hat{\Psi}_{rI}^s \right) dt \geq -\gamma_1^2$ (12)

$S_2 = \int_0^{t_1} \Delta R_S \left(\underline{\varepsilon}_V^T . i_s^s \right) dt \geq -\gamma_2^2$ (13)

$\hat{\omega} = \left(K_{p\omega} + \frac{K_{I\omega}}{p} \right) \left(\underline{\varepsilon}_I^T . J . \hat{\Psi}_{rI}^s \right) = \left(K_{p\omega} + \frac{K_{I\omega}}{p} \right) e_\omega$ (14)

$\hat{R}_s = \left(K_{pR_s} + \frac{K_{IR_s}}{p} \right) \left(\underline{\varepsilon}_V^T . i_s^s \right) = \left(K_{pR_s} + \frac{K_{IR_s}}{p} \right) e_{R_s}$ (15)

Where $K_{p\omega}$, $K_{I\omega}$, K_{pR_s}, K_{IR_s}, are PI controller parameters of rotor speed and stator resistance, adaptation mechanisms, respectively. The value of $\boldsymbol{\underline{\varepsilon}_I^T . J . \hat{\Psi}_{rI}^s}$ in (12), (14) is evaluated by taking into account that, for speed estimation, the output of the reference model (1) is taken as equal to the true rotor flux space vector. Hence $\underline{\varepsilon}_I = \underline{\Psi}_{rI}^s - \underline{\hat{\Psi}}_{rI}^s = \underline{\hat{\Psi}}_{rV}^s - \underline{\hat{\Psi}}_{rI}^s$,

since $\underline{\Psi}_{rI}^s \equiv \underline{\hat{\Psi}}_{rV}^s$,

Thus

$$\underline{\varepsilon}_I^T . J . \hat{\Psi}_{rI}^s = \left[\hat{\Psi}_{\alpha rV} - \hat{\Psi}_{\alpha rI} \quad \hat{\Psi}_{\beta rI} - \hat{\Psi}_{\beta rV} \right] . \begin{bmatrix} 0 & -1 \\ 1 & 0 \end{bmatrix} . \begin{bmatrix} \hat{\Psi}_{\alpha rI} \\ \hat{\Psi}_{\beta rI} \end{bmatrix}$$

$$= \left[\hat{\Psi}_{\alpha rV} - \hat{\Psi}_{\alpha rI} \quad \hat{\Psi}_{\beta rI} - \hat{\Psi}_{\beta rV} \right] . \begin{bmatrix} \widehat{-\Psi}_{\beta rI} \\ \hat{\Psi}_{\alpha rI} \end{bmatrix}$$

$$= \underline{\hat{\Psi}}_{rI} X \underline{\hat{\Psi}}_{rV} = e_\omega(t) \quad (16)$$

The error quantity for speed estimation is therefore the one of (4). The value of $\boldsymbol{\underline{\varepsilon}_V^T . i_s^s}$ in (13), (15) needs to be evaluated next. In order to do this, it is necessary to take into account that, for stator resistance estimation, reference and adjustable model (1), (2) change the roles. The true value of the rotor flux space vector is now taken to be the output of (2).

Hence $\underline{\varepsilon}_V = \underline{\Psi}_{rV}^s - \underline{\hat{\Psi}}_{rV}^s = \underline{\hat{\Psi}}_{rI}^s - \underline{\hat{\Psi}}_{rV}^s$,

since $\underline{\Psi}_{rV}^s \equiv \underline{\hat{\Psi}}_{rI}^s$.

One further has

$$-\underline{\varepsilon}_V^T . i_s^s = \left[\hat{\Psi}_{\alpha rV} - \hat{\Psi}_{\alpha rI} \quad \hat{\Psi}_{\beta rV} - \hat{\Psi}_{\beta rI} \right] . \begin{bmatrix} \hat{\Psi}_{\alpha rI} \\ \hat{\Psi}_{\beta rI} \end{bmatrix}$$

$$= i_{\alpha s} \left(\hat{\Psi}_{\alpha rV} - \hat{\Psi}_{\alpha rI} \right) + i_{\beta s} \left(\hat{\Psi}_{\beta rV} - \hat{\Psi}_{\beta rI} \right)$$

$$= i_s^S \left(\underline{\Psi}_{rV} - \underline{\Psi}_{rI} \right) = e_{R_s}(t) \quad (17)$$

The error quantity for stator resistance estimation is therefore

$e_{R_s} = i_{\alpha s} \left(\hat{\Psi}_{\alpha rV} - \hat{\Psi}_{\alpha rI} \right) + i_{\beta s} \left(\hat{\Psi}_{\beta rV} - \hat{\Psi}_{\beta rI} \right)$ (18)

It follows from these considerations that the role of the reference and the adjustable models is interchangeable in the parallel system of rotor speed and stator resistance estimation. The speed and stator resistance can be estimated in parallel using (14), (15) at any speed. The rotor speed adaptation mechanism (14) is the same as in the customary MRAS speed estimator reviewed in Section II. Stator resistance adaptation mechanism (15) is, at the first sight, similar to the one of [17, 18]. However, stator resistance is here estimated in the stationary reference frame (rather than in the rotor flux oriented reference frame), and error quantity is obtained using two rotor flux space vector estimates (rather than the reference and a single estimated value, as in [18]). Further, stator resistance and rotor speed estimation operate in parallel, rather than sequentially as in [19]. This is enabled by utilizing the second available degree of freedom (the difference in rotor flux amplitudes) in the process of stator resistance estimation.

RESULTS

1. Simulation Results

In this section the simulation results is discussed for the proposed method. The key parameters are listed in Table 1. MATLAB/Simulink software used to verify the influence of the MRAS controller with and without stator resistance tuning. Fig. 5 shows that performance of speed and torque response for without stator resistance compensation. Due to temperature variation at low frequency it is well known that stator resistance is a changeable parameter during motor operation. In order to estimate correct speed, we need to identify the stator resistance in real time. Fig. 6 shows a sample of simulation results on stator resistance identification under the condition of constant speed reference. In this simulation, the initial value of the stator resistance was 0.1Ω (20% increased value of Rs) and a convergence characteristic of stator resistance according to time *t=1s* was investigated. We can see some mismatches between speed reference and estimated speed for a couple of seconds in Fig. 6. This is a result of stator resistance estimation errors. However, it does not matter because the thermal time constant of stator resistance is large enough for correct estimation. Moreover, we estimated it from the instant the motor started. Fig. 7 represents a simulation results for stator resistance identification under the condition of variable speed reference. We can see that the estimated rotor resistance converges to a real value after a few seconds.

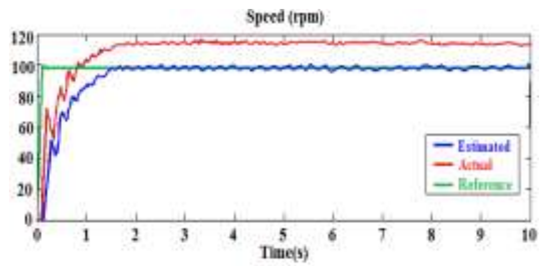

(a)

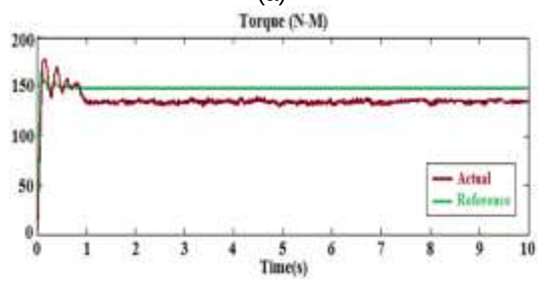

(b)

Fig.5 Simulation results without Rs compensation (a) Rotor Speed (100rpm) (b) Torque

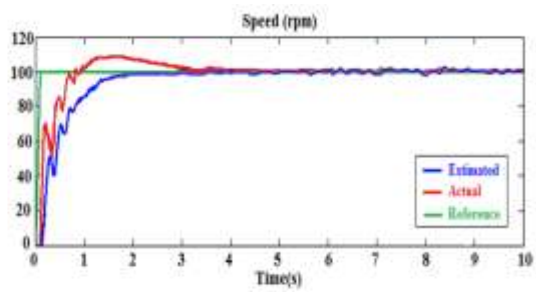

(a)

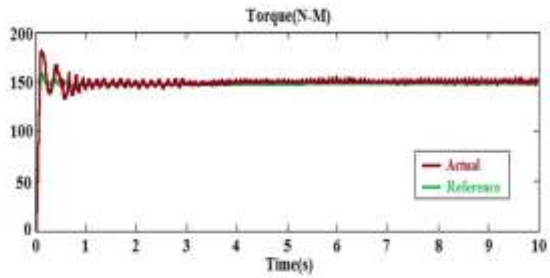

(b)

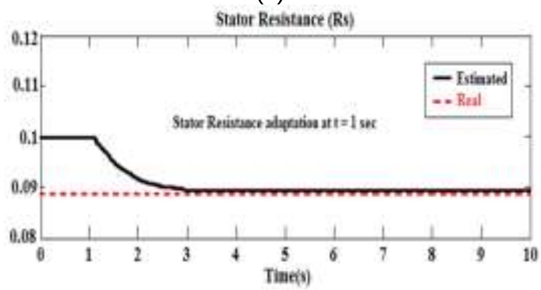

(c)

Fig.6 Simulation results (a) Rotor Speed (b) Torque response (c) Rs Estimation(=1.2*Rs)

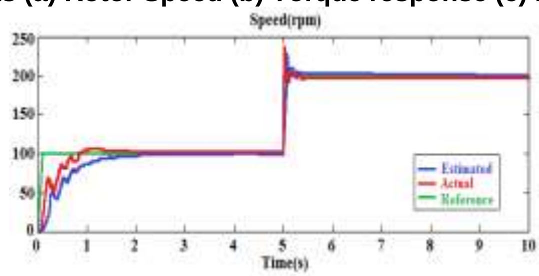

(a)

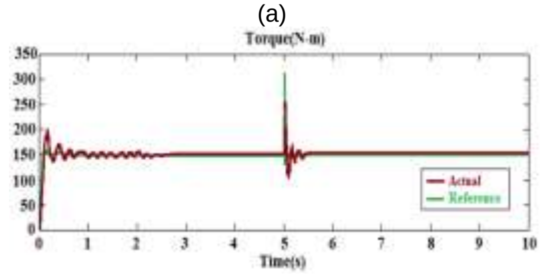

Fig.7 Simulation results (a) Step Speed response (100 to 200rpm) (b) Torque response with Rs compensation

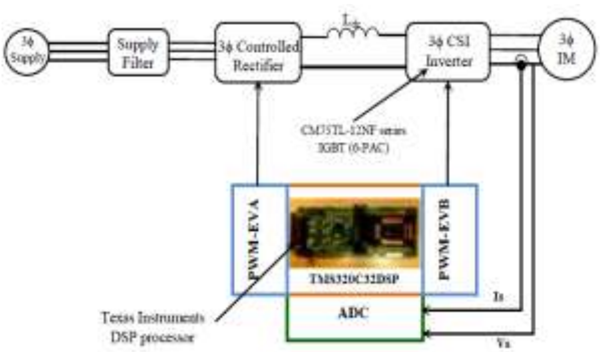

Fig.– 8 Experimental setup

2. Experimental Results:

An experimental system is constructed for verification with key parameters listed in Table 2. A dc motor is coupled to the shaft of the induction machine under the test it was used as the load machine to generate the load torque. Experiments were obtained using a DSP TMS320C32 from Texas Instruments Incorporated. All measured internal variables of controller are accessible through the serial link to the PC, where graphical data-analysis software can be run. The sampling time of the measurements and computation of the control algorithm are both 200 μs.

The control of both speed and applied torque is possible, thus, a hardware-in-the-loop operation can also be performed (Fig. 8).

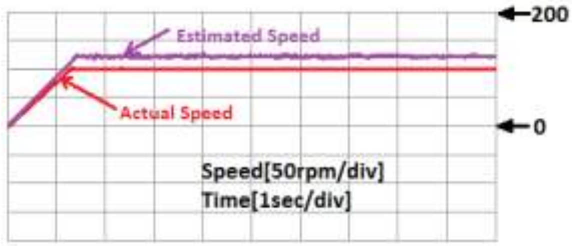

(a)

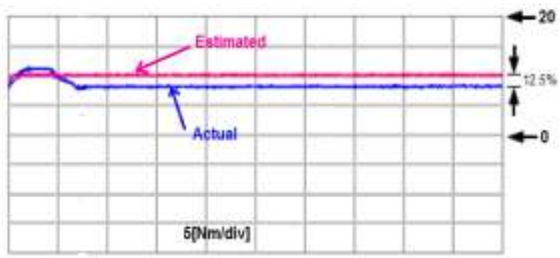

(b)

Fig 9 Experimental results without Rs compensation (a) Rotor Speed (ramp input) with 100rpm (b)Torque response

Fig. 9 represents the experimental results of the Speed and torque performance of the IM without stator resistance compensation. In order to test the effect of stator resistance variations on the estimated speed and torque were intentionally changed to their actual value. The same experiment was repeated using the stator resistance compensation in the testing system as shown in Fig 10. Here, the estimated speed Fig. 10(a) and torque Fig. 10(b) delivered from the controller to compensate the parameter variation effects. The speed and torque error was nearly reduced to zero Fig. 10(c) shows estimated stator resistance using (15). It shows an excellent convergence characteristic from the initial value with some initial errors to the real value after a few seconds. The estimated speed coincides with the actual speed even in the state of a load torque addition. The torque response in the Fig. 10(b) was confirmed by the actual torque from toque-meter (T/M) installed on the motor shaft. The tests were performed with and without load torque command in the test motor. Fig. 11 shows that the experimental results of the speed sensorless control without load torque.

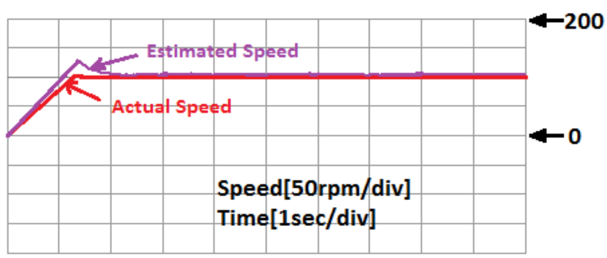

(a)

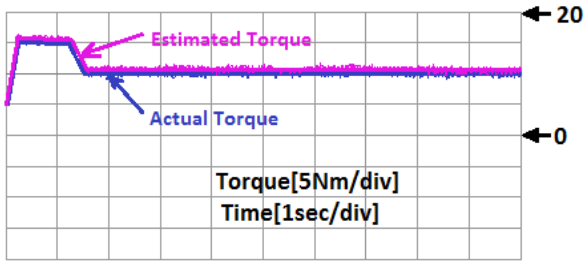

(b)

(c)

Fig.10 Experimental results with load (a) Speed reponse(Ramp input) (b) Torque response (c) Rs Estimation(=1.5*Rs)

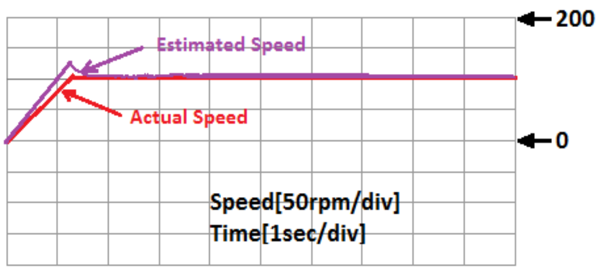

(a)

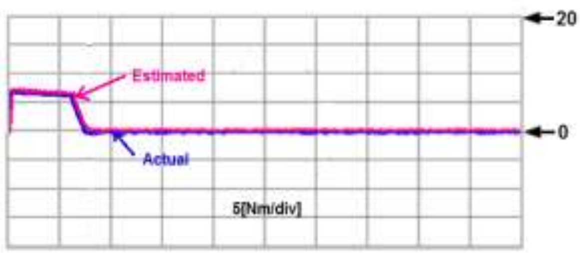

(b)

Fig.11 Experimental results without load (a) Speed response(Ramp input) (b) Torque response

Table I Induction motor parameters (Simulation)

Rated Power	50 hp	Mutual Inductance	34.7mH
Rated Voltage	460 V	Moment of inertia	1.662kg.m^2
Stator Resistance	0.087 Ω	Friction co efficient	0.1N.m.s/rad
Rotor Resistance	0.228 Ω	Number of poles	4
Stator Inductance	5.5 mH	Inverter side capacitor	500 µF
Rotor Inductance	5.5 mH	DC inductance	35mH

Table II Induction motor parameters (Experimental)

Rated Power	3 hp	Mutual Inductance	69.31mH
Rated Voltage	220 V	Moment of inertia	0.089kg.m^2
Stator Resistance	0.435 Ω	Friction co efficient	0.005N.m/s
Rotor Resistance	0.816 Ω	Number of poles	4
Stator Inductance	2 mH	Inverter side capacitor	500 μF
Rotor Inductance	2 mH	DC inductance	35mH

CONCLUSIONS

A proposed method of MRAS estimator enables simultaneous estimation of rotor speed and stator resistance. Very first time the proposed this method has been applied to CSI fed FOC induction motor drive without speed sensor. The parallel adaptive approach is used to identify *Rs* to enhance the robustness of the sensorless FOC-IM drive in the range of low speed. The proposed estimator can estimate the stator resistance over a wide range of resistance variation due to temperature and frequency changes. The structure of the estimator is derived using hyper stability theory and it utilizes both degrees of freedom, available within the standard rotor flux based MRAS speed estimator. The error in the instantaneous phase position of the two rotor flux estimates is utilized for rotor speed identification, this being the same as in the standard approach. The second degree of freedom, the error in the amplitudes of the two rotor flux estimates, is used for parallel stator resistance estimation. The proposed parallel MRAS system is insignificantly more complex than its counterpart with speed estimation only and it enables very good speed estimation accuracy down to very low speeds or zero speed. The effectiveness of the developed parallel MRAS structure is verified by simulation and experimental at low-speed region. The proposed estimator can estimate the stator resistance over wide range resistance variations due to temperature and frequency changes. The estimation error of speed and stator resistance is very small and the speed response is adequate for variable speed drives. The capability of the drive to operate at zero speed and the simulation and experimental results show that the CSI fed FOC induction motor with MRAS controller with stator resistance tuning works well at low speed with promising the good speed performance.

REFERENCES

1. Y.W. Li, M. Pande, N. R. Zargari, and B.Wu, *"Dc-link current minimization for high-power current-source motor drives," IEEE Trans. Power Electron.*, vol. 24, no. 1, pp. 232–240, Jan. 2009.
2. Weber, P. Kern, and T. Dalibor*, "A novel 6.5 kV IGCT for high power current source inverters,"* in *Proc. Int. Symp. Power Semicond. Devices ICs*, Osaka, Japan, 2001, pp. 215–218.
3. N.R. Zargari, S.C.Rizzo,Y.Xiao,H. Iwamoto,K. Satoh, and J. F.Donlon, *"A new current-source converter using a symmetric gate-commutated thyristor (SGCT)," IEEE Trans. Ind. Appl.*, vol. 37, no. 3, pp. 896–903, May/Jun. 2001.
4. Y. W. Li, M. Pande, N. R. Zargari, and B. Wu*, "An input power factor control strategy for high-power current-source induction motor drive with active front-end," IEEE Trans. Power Electron.*, vol. 25, no. 2, pp. 352– 359, Feb. 2010.
5. J.D.Ma, B.Wu,N. R. Zargari, and S. C. Rizzo, *"A space vector modulated CSI-based ac drive for multi motor applications," IEEE Trans. Power Electron.*, vol. 16, no. 4, pp. 535–544, Jul. 2001.
6. A.Klonne and F.W. Fuchs, *"High dynamic performance of a PWM current source converter induction machine drive,"* in *Proc. 10th Eur. Conf. Power Electron. Appl.*, 2003, pp. 1–10.
7. V. D. Colli, P. Cancelliere, F. Marignetti, and R. D. Stefano, "*Influence of voltage and current source inverters on low-power induction motors," IEE Proc. Electr. Power Appl.*, vol. 152, no. 5, pp. 1311–1320, Sep. 2005.
8. M. Salo andH. Tuusa, *"A vector-controlled PWM current-source-inverter fed induction motor drive with a new stator current control method," IEEE Trans. Ind. Electron.*, vol. 52, no. 2, pp. 523–531, Apr. 2005.
9. G. O. Garcia, R. M. Stephan, and E. H.Watanabe, *"Comparing the indirect field-oriented control with a scalar method," IEEE Trans. Ind. Electron.*, vol. 41, pp. 201–207, Apr. 1994.
10. Arul Prasanna Mark, Gerald Christopher Raj Irudayaraj, Rajasekaran Vairamani, and Kaliamoorthy Mylsamy, *"Dynamic Performance Analysis for Different Vector-Controlled CSI- Fed Induction Motor Drives"*, Journal of Power Electronics, vol. 14, no. 5, pp. 989-999, September 2014.
11. M. P. Kazmierkowski and A. B. Kasprowicz*, "Improved direct torque and flux vector control of PWM inverter-fed induction motor drives," IEEE Trans. Ind. Electron.*, vol. 42, pp. 344–350, Aug. 1995.
12. N.Panneer selvam, V.Rajasekaran, M.Arul Prasanna, and I.Gerald Christopher, "*High performance sensorless DTC-CSI fed Induction motor drive for low speed operation with minimum ripple torque*" International review of Electrical Engineering, vol.9, no.2, pp 315-321. Apr-2014.
13. R. Marino, S. Peresada, and P. Tomei, *"On-line stator and rotor resistance estimation for induction motors," IEEE Trans. Contr. Syst. Technol.*, vol. 8, pp. 570–579, May 2000.

14. T. G. Habetler, F. Profumo, G. Griva, M. Pastorelli, and A. Bettini, *"Stator resistance tuning in a stator-flux field-oriented drive using an instantaneous hybrid flux estimator," IEEE Trans. on Power Electronics,* vol. 13, no. 1, pp. 125-133, 1998.
15. I.J.Ha, and S.H.Lee, *"An online identification method for both stator and rotor resistance of induction motors without rotational transducers," IEEE Trans. on Industrial Electronics,* vol. 47, no. 4, pp. 842-853, 2000.
16. M. Tsuji, S. Chen, K. Izumi, and E. Yamada, *"A sensorless vector control system for induction motors using q-axis flux with stator resistance identification," IEEE Trans. on Industrial Electronics,* vol. 48, no. 1, pp. 185-194, 2001.
17. K.Akatsu, and A.Kawamura, *"Sensorless very low-speed and zero-speed estimations with online rotor resistance estimation of induction motor without signal injection," IEEE Trans. on Industry Applications,* vol. 36, no. 3, pp. 764-771, 2000.
18. N. Panneer Selvam, V.Rajasekaran,*"High Performance Operation of DTC-CSI Fed IM Drives at Low Speed with On-Line Stator Resistance compensation",* International Journal of Applied Engineering Research, vol 9, no.23, Apr-2014 pp. 19211-19230.
19. L.Zhen, and L.Xu*, "Sensorless field orientation control of induction machines based on a mutual MRAS scheme," IEEE Trans. on Industrial Electronics,* vol. 45, no. 5, pp. 824-831, 1998.
20. C.Schauder, *"Adaptive speed identification for vector control of induction motors without rotational ransducers," IEEE Trans. On Industry Applications,* vol. 28, no. 5, pp. 1054-1061, 1992.

Author' biography with Photo

N.**Panneer Selvam** was born in 05th May 1969. He has received his B.E., in Electrical and Electronics Engineering from Madurai Kamaraj University, Madurai, TamilNadu in the year 1995, M.E., in Power Electronics and Drives from Anna University, Chennai, TamilNadu in the year 2009 and pursuing Ph.D., in Power Electronics and Drives Anna University, Trichyi, TamilNadu. His research interest includes Power Electronics and Drives, Current Source Inverters, AC drives and application and Power Electronics converters. He is a Life member of the Indian Society for Technical Education (ISTE). Currently he is working as a Principal in M.A.M. Polytechnic College,Trichirappalli, TamilNadu, India.

Dr. V. Rajasekaran was born in Madurai, Tamilnadu, India in 1971. He received his BE (Electrical and Electronics Engg) in 1994, ME (Power Systems) in 1997, and PhD in 2007 from Madurai Kamaraj University, Madurai, India. He is now heading the Electrical and Electronics Department, PSNA CET, Dindigul, Tami lnadu, India. He is a certified Energy auditor. His field of interest are Power Systems, Energy, Power Quality.